

The effects of a magnetic barrier and a nonmagnetic spacer in tunnel structures

This article has been downloaded from IOPscience. Please scroll down to see the full text article.

2004 J. Phys.: Condens. Matter 16 4455

(<http://iopscience.iop.org/0953-8984/16/25/006>)

[View the table of contents for this issue](#), or go to the [journal homepage](#) for more

Download details:

IP Address: 129.252.86.83

The article was downloaded on 27/05/2010 at 15:37

Please note that [terms and conditions apply](#).

The effects of a magnetic barrier and a nonmagnetic spacer in tunnel structures

Ali A Shokri¹ and Alireza Saffarzadeh^{2,3}

¹ Department of Physics, Sharif University of Technology, 11365-9161, Tehran, Iran

² Department of Physics, Tehran Payame Noor University, Fallahpour Street, Nejatollahi Street, Tehran, Iran

E-mail: aashokri@mehr.sharif.edu and a-saffar@tehran.pnu.ac.ir

Received 24 February 2004

Published 11 June 2004

Online at stacks.iop.org/JPhysCM/16/4455

doi:10.1088/0953-8984/16/25/006

Abstract

The spin-polarized transport is investigated in a new type of magnetic tunnel junction which consists of two ferromagnetic electrodes separated by a magnetic barrier and a nonmagnetic metallic spacer. Based on the transfer matrix method and the nearly-free-electron approximation the dependence of the tunnel magnetoresistance (TMR) and electron-spin polarization on the nonmagnetic layer thickness and the applied bias voltage are studied theoretically. The TMR and spin polarization show an oscillatory behaviour as a function of the spacer thickness and the bias voltage. The oscillations originate from the quantum well states in the spacer, while the existence of the magnetic barrier gives rise to a strong spin polarization and high values of the TMR. Our results may be useful for the development of spin electronic devices based on coherent transport.

1. Introduction

During recent years, the large magnetoresistance of magnetic tunnel junctions (MTJs) has attracted much attention due to the possibility of its application in digital storage and magnetic sensor technologies [1, 2]. In most of the experiments, the MTJs consist of two ferromagnetic metal (FM) electrodes separated by a thin insulator (FM/I/FM). In these structures, the electrical resistance is reduced when the magnetization direction of the FM layers changes from antiparallel to parallel alignment by an external magnetic field. Because the tunnel magnetoresistance (TMR) strongly depends on the spin polarization of the magnetic electrodes [3, 4], attempts have been made to fabricate junctions with more highly spin-polarized ferromagnets [5, 6].

³ Author to whom any correspondence should be addressed.

Recent experiments on the TMR have shown that the insertion of a thin nonmagnetic metal (NM) layer between insulating barrier and the FM electrode (FM/I/NM/FM) reduces the TMR, when the thickness of the NM layer increases [7–10]. This decrease of the TMR can be attributed to the decoherence tunnelling of electrons from one electrode to the other through the NM layer [11]. On the other hand, recent observations by Yuasa *et al* [12] show clear oscillations of the TMR in high-quality NiFe/Al₂O₃/Cu/Co junctions in which the Cu/Co is a single crystal. This oscillatory behaviour has been interpreted in terms of the formation of spin-polarized resonant tunnelling.

The effect of nonmagnetic metallic interlayers has been theoretically investigated in FM/NM/I/NM/FM structures. Based on the Kubo formalism, Vedyayev *et al* [13] studied magnetoconductivity as a function of NM layer thickness at low bias voltages. By using the transfer matrix approach, Wilczyński and Barnaś [14] calculated the thickness and voltage dependence of TMR. These calculations showed that the presence of thin NM spacers can lead to the formation of quantum well states that lead to oscillations of magnetoconductivity and TMR. When the thickness of only one of the NM layer varies, and also in the case of an asymmetric structure, such as FM/NM/I/FM [15], the sign of magnetoconductivity and TMR is predicted to oscillate as a function of the NM layer thickness.

TMR has also been investigated both experimentally [16, 17] and theoretically [18–21] in spin filter tunnel junctions in which a ferromagnetic semiconductor (FMS) is applied as a magnetic barrier. The large spin polarization achievable using magnetic barriers [22] makes spin filtering a nearly ideal method for spin injection into semiconductors, enabling novel spintronic devices [23]. When an FMS layer which acts as a spin filter is used in tunnel structures, due to the spin splitting of its conduction band, tunnelling electrons see a spin-dependent barrier height. Thus one spin channel will have a larger tunnelling probability than the other, and a highly spin-polarized current may result.

The purpose of the present work is to investigate theoretically the effect of a magnetic barrier on spin transport in the presence of a nonmagnetic spacer layer. Using the transfer matrix method and the nearly-free-electron approximation we will study the variation of TMR and spin polarization of tunnelling electrons in terms of the spacer thickness and bias voltage at $T = 0$ K. We assume that the electron wavevector parallel to the interfaces and the electron spin are conserved in the tunnelling process through the whole system.

The paper is organized as follows. In section 2, the model and the analytic formulae of the spin polarization and TMR for FM/FMS/NM/FM structure are presented. In section 3, numerical results obtained for a typical tunnel junction are discussed. The results of this work are summarized in section 4.

2. Description of model and formalism

We consider two semi-infinite FM electrodes separated by a ferromagnetic barrier which acts as a spin filter, and a nonmagnetic metallic layer as a quantum well, in the presence of DC applied bias V_a as shown in figure 1. For simplicity, we assume that the two FM electrodes are made of the same metal and all of the interfaces are flat. In the nearly-free-electron approximation of spin-polarized conduction electrons, the longitudinal part of the effective one-electron Hamiltonian can be written as

$$H_x = -\frac{\hbar^2}{2m_j^*} \frac{d^2}{dx^2} + U_j(x) - \mathbf{h}_j \cdot \boldsymbol{\sigma} + V^\sigma, \quad (1)$$

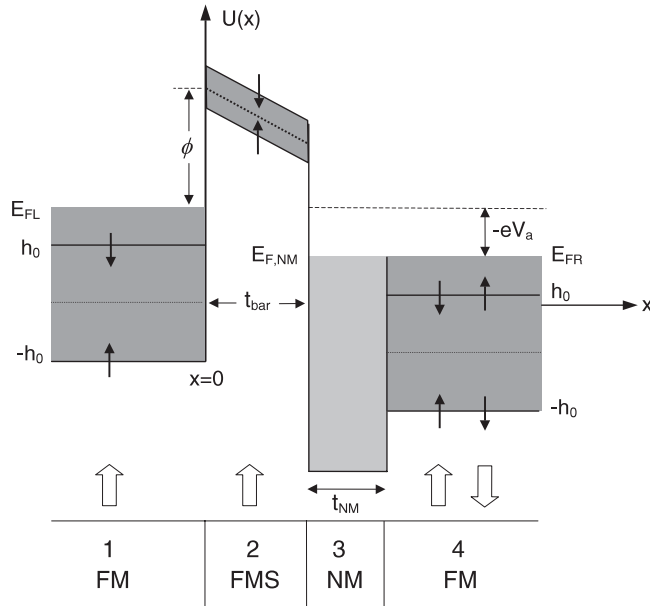


Figure 1. Spin-dependent potential profile for an FM/FMS/NM/FM magnetic tunnel junction under forward bias V_a . In the FMS layer, the dashed line represents the bottom of the conduction band at $T \geq T_c$ and the thin arrows indicate the bottom of the conduction band for spin-up and spin-down electrons at $T < T_c$. The zero of energy is taken at the middle of the bottoms for the majority-spin band and minority-spin one in the left FM electrode.

where m_j^* ($j = 1\text{--}4$) is the electron effective mass in the j th layer, and

$$U_j(x) = \begin{cases} 0, & x < 0, \\ E_{FL} + \phi - eV_a x / t_{bar}, & 0 < x < t_{bar}, \\ -eV_a, & t_{bar} < x < t_{bar} + t_{NM}, \\ -eV_a, & x > t_{bar} + t_{NM}, \end{cases} \quad (2)$$

where E_{FL} is the Fermi energy in the left electrode. $-\mathbf{h}_j \cdot \boldsymbol{\sigma}$ is the internal exchange energy where \mathbf{h}_j is the molecular field in the j th FM electrode and $\boldsymbol{\sigma}$ is the conventional Pauli spin operator. The last term in equation (1) is a spin-dependent potential and denotes the s-f exchange coupling between the spin of tunnelling electrons and the localized f spins in the magnetic barrier. This term, within the mean-field approximation, is proportional to the thermal average of the f spins, $\langle S_z \rangle$, and can be written as $V^\sigma = -\sigma I \langle S_z \rangle$. Here, $\sigma = \pm 1$ which corresponds to $\sigma = \uparrow, \downarrow$, and I is the s-f exchange constant in the magnetic barrier.

The Schrödinger equation for a biased barrier layer can be simplified by a coordinate transformation whose solution is the linear combination of the Airy function $Ai[\rho(x)]$ and its complement $Bi[\rho(x)]$ [24]. Considering all four regions of the FM/FMS/NM/FM junction shown in figure 1, the eigenfunctions of the Hamiltonian (1) with eigenvalue E_x have the following forms:

$$\psi_{j,\sigma}(x) = \begin{cases} A_{1\sigma} e^{ik_{1\sigma}x} + B_{1\sigma} e^{-ik_{1\sigma}x}, & x < 0, \\ A_{2\sigma} Ai[\rho_\sigma(x)] + B_{2\sigma} Bi[\rho_\sigma(x)], & 0 < x < t_{bar}, \\ A_{3\sigma} e^{ik_{3\sigma}x} + B_{3\sigma} e^{-ik_{3\sigma}x}, & t_{bar} < x < t_{bar} + t_{NM}, \\ A_{4\sigma} e^{ik_{4\sigma}x} + B_{4\sigma} e^{-ik_{4\sigma}x}, & x > t_{bar} + t_{NM}, \end{cases} \quad (3)$$

where

$$k_{1\sigma} = \sqrt{2m_1^*(E_x + h_0\sigma)/\hbar}, \quad (4)$$

$$k_3 = \sqrt{2m_3^*(E_x + eV_a + E_{F,NM} - E_{FL})/\hbar}, \quad (5)$$

$$k_{4\sigma} = \sqrt{2m_4^*(E_x + eV_a + \eta h_0\sigma)/\hbar}, \quad (6)$$

are the electron wavevectors along the x axis. Here, $h_0 = |\mathbf{h}_j|$ and $\eta = +1$ (-1) for parallel (antiparallel) alignment of the magnetizations. The coefficients $A_{j\sigma}$ and $B_{j\sigma}$ are constants to be determined from the boundary conditions, while

$$\rho_\sigma(x) = \frac{x}{\lambda} + \beta_\sigma, \quad (7)$$

with

$$\lambda = \left[-\frac{\hbar^2 t_{\text{bar}}}{2m_2^* e V_a} \right]^{1/3}, \quad (8)$$

$$\beta_\sigma = \frac{[E_x - E_{FL} - \phi_{\text{bar}} - V^\sigma]t_{\text{bar}}}{eV_a\lambda}. \quad (9)$$

Although the transverse momentum \mathbf{k}_\parallel is omitted from the above notations, the summation over \mathbf{k}_\parallel is carried out in our calculations.

Upon applying the boundary conditions such that the wavefunctions and their first derivatives are matched at each interface point x_j , i.e. $\psi_{j,\sigma}(x_j) = \psi_{j+1,\sigma}(x_j)$ and $(m_j^*)^{-1}[\text{d}\psi_{j,\sigma}(x_j)/\text{d}x] = (m_{j+1}^*)^{-1}[\text{d}\psi_{j+1,\sigma}(x_j)/\text{d}x]$, we obtain a matrix formula that connects the coefficients $A_{1\sigma}$ and $B_{1\sigma}$ with the coefficients $A_{4\sigma}$ and $B_{4\sigma}$ as follows:

$$\begin{bmatrix} A_{1\sigma} \\ B_{1\sigma} \end{bmatrix} = M_{\text{total}} \begin{bmatrix} A_{4\sigma} \\ B_{4\sigma} \end{bmatrix}, \quad (10)$$

where

$$\begin{aligned} M_{\text{total}} = \frac{k_{4\sigma}}{k_{1\sigma}} & \begin{bmatrix} ik_{1\sigma} & \frac{1}{\lambda} \frac{m_1^*}{m_2^*} \\ ik_{1\sigma} & -\frac{1}{\lambda} \frac{m_1^*}{m_2^*} \end{bmatrix} \begin{bmatrix} \text{Ai}[\rho_\sigma(x=0)] & \text{Bi}[\rho_\sigma(x=0)] \\ \text{Ai}'[\rho_\sigma(x=0)] & \text{Bi}'[\rho_\sigma(x=0)] \end{bmatrix} \\ & \times \begin{bmatrix} \text{Ai}[\rho_\sigma(x=t_{\text{bar}})] & \text{Bi}[\rho_\sigma(x=t_{\text{bar}})] \\ \frac{1}{\lambda} \frac{1}{m_2^*} \text{Ai}'[\rho_\sigma(x=t_{\text{bar}})] & \frac{1}{\lambda} \frac{1}{m_2^*} \text{Bi}'[\rho_\sigma(x=t_{\text{bar}})] \end{bmatrix}^{-1} \\ & \times \begin{bmatrix} \cos(k_3 t_{\text{NM}}) & -\frac{m_3^*}{k_3} \sin(k_3 t_{\text{NM}}) \\ \frac{k_3}{m_3^*} \sin(k_3 t_{\text{NM}}) & \cos(k_3 t_{\text{NM}}) \end{bmatrix} \begin{bmatrix} ik_{4\sigma} & m_4^* \\ ik_{4\sigma} & -m_4^* \end{bmatrix}^{-1} \\ & \times \begin{bmatrix} e^{-ik_{4\sigma}(t_{\text{bar}}+t_{\text{NM}})} & 0 \\ 0 & e^{ik_{4\sigma}(t_{\text{bar}}+t_{\text{NM}})} \end{bmatrix}^{-1}. \end{aligned} \quad (11)$$

Since there is no reflection in region 4, the coefficient $B_{4\sigma}$ in equation (3) is zero and the transmission coefficient (TC) of the spin σ electron, which is defined as the ratio of the transmitted flux to the incident flux, can be written as

$$T_\sigma(E_x, V_a) = \frac{k_{4\sigma} m_1^*}{k_{1\sigma} m_4^*} \left| \frac{1}{M_{\text{total}}^{11}} \right|^2, \quad (12)$$

where M_{total}^{11} is the left-upper element of the matrix M_{total} defined in equation (11). At $T = 0$ K, the spin-dependent current density for the magnetic tunnel junction at a given applied bias V_a within the nearly-free-electron model is given by the formula [25]

$$J_\sigma(V_a) = \frac{em_1^*}{4\pi^2 \hbar^3} \left[eV_a \int_{E_0^\sigma}^{E_{FL}-eV_a} T_\sigma(E_x, V_a) \text{d}E_x + \int_{E_{FL}-eV_a}^{E_{FL}} (E_{FL} - E_x) T_\sigma(E_x, V_a) \text{d}E_x \right], \quad (13)$$

where E_0^σ is the lowest possible energy that will allow transmission and is given by $E_0^\uparrow = \max\{-h_0, -eV_a - \eta h_0\}$ for spin-up and $E_0^\downarrow = h_0$ for spin-down electrons. It is clear that the tunnel current is modulated by the magnetic configurations of both the FM electrodes.

The degree of spin polarization for the tunnel current is defined by

$$P = \frac{J_\uparrow - J_\downarrow}{J_\uparrow + J_\downarrow}, \quad (14)$$

where J_\uparrow (J_\downarrow) is the spin-up (spin-down) current density. For the present structure, we obtain this quantity when the magnetizations of two FM electrodes and the FMS layer (magnetic barrier) are in parallel alignment. For calculating the TMR, both the spin currents in the parallel and antiparallel alignments are calculated. In this case, the TMR can be defined as

$$\text{TMR} = \frac{(J_\uparrow^P + J_\downarrow^P) - (J_\uparrow^{AP} + J_\downarrow^{AP})}{J_\uparrow^{AP} + J_\downarrow^{AP}}, \quad (15)$$

where $J_{\uparrow,\downarrow}^{P(AP)}$ corresponds to the current density in the parallel (antiparallel) alignments of the magnetizations in the FM electrodes, for a spin-up (\uparrow) or spin-down (\downarrow) electron.

3. Numerical results and discussion

Numerical calculations have been carried out to investigate the effect of a magnetic barrier and an NM metallic layer on the spin transport in the Fe/EuS/Au/Fe structure as a typical MTJ. We have chosen Fe and EuS because they have cubic structures and the lattice mismatch is very small [26]. The parameters E_F and h_0 for Fe electrodes are taken corresponding to $k_{F\uparrow} = 1.09 \text{ \AA}^{-1}$ and $k_{F\downarrow} = 0.42 \text{ \AA}^{-1}$ (for itinerant d electrons) [27]. For the EuS layer we use $S = 7/2$, $I = 0.1 \text{ eV}$ [28], $\phi = 1.94 \text{ eV}$ [21] as a symmetric barrier height, and $t_{\text{bar}} = 1.3788 \text{ nm}$ which corresponds to four monolayers of EuS(111) [29]. The Fermi energy in the Au layer is $E_{F,\text{NM}} = 5.51 \text{ eV}$ [30]. In practice, the effective masses of electrons may differ from that of the free electron, but here for simplicity we assume that all electrons have the same mass, m_e , as free electrons.

In our considered system, the magnetization direction of the left Fe electrode and the EuS magnetic barrier stays fixed, because they are coupled through the interface. Inserting the NM spacer layer between the FMS layer and the right FM electrode decreases the exchange coupling between the two FM electrodes. Therefore the right Fe electrode is free and may be switched back and forth by an external magnetic field (see figure 1). In the following, we show the numerical results at $T = 0 \text{ K}$, so in the magnetic barrier we have $\langle S_z \rangle = S$.

The TC for tunnelling electrons at the Fermi energy, and the TMR in the tunnel junction as a function of the NM layer thickness are shown in figures 2(a) and (b), respectively. It can be seen that both the TC and the TMR oscillate with the NM layer thickness due to the dependence of these quantities on the incident electron's energy and the NM layer thickness. The physics behind this behaviour is easy to understand. When the energy of the incident electrons is approximately equal to the energy of a quasibound state in the quantum well, a resonance condition is fulfilled and the TC of the electrons through the structure strongly increases. On the other hand, the position of the quantum well levels, formed in the NM layer, strongly depends on the well thickness. Therefore, with continuous variation of the t_{NM} , the position of the resonant states varies and this leads to the oscillations of the TC and the TMR. From figure 2, it is clear that where the transmission is high, the TMR is low. From the continuous variation of t_{NM} , one can see that both the TC and the TMR oscillate with a period of 0.26 nm, which is in excellent agreement with $\lambda_F/2$, where λ_F is the Fermi wavelength in the Au layer and is equal to 0.522 nm. The results show that, for the spin-up electrons, the

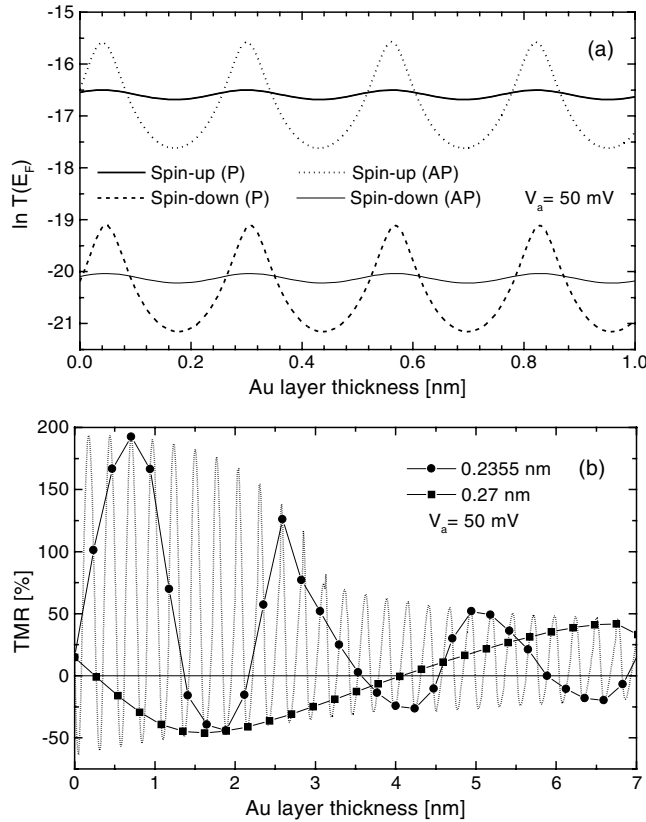


Figure 2. (a) Spin-dependent TC at Fermi energy in the parallel (P) and antiparallel (AP) configurations, and (b) dependence of the TMR, as a function of Au layer thickness.

TC is much higher than the spin-down ones both in the parallel and antiparallel alignment of magnetizations. The reason can be explained by the spin filtering effect of the FMS barrier. As shown in figure 1, due to the spin splitting of the conduction band in the FMS layer, the barrier height for spin-up electrons is lowered and the tunnelling probability greatly increases, while for the spin-down electrons the barrier height is raised, and hence the tunnelling probability for these electrons reduces. Thus, a large spin-polarized current is produced.

In figure 2(b) we have also shown the TMR in terms of thickness, when t_{NM} changes in monolayer steps. At the monolayer thickness $t_{ML,NM} = 0.2355$ nm, which corresponds to the interlayer distance of Au(111), the TMR first increases in the first three monolayer and after that the TMR becomes less and starts to oscillate with a period of approximately 2.5 nm. In contrast, for $t_{ML,NM} = 0.27$ nm, the TMR initially decreases and the period of oscillations is approximately 7 nm.

The voltage dependence of the TMR for several thicknesses is shown in figure 3, when $t_{ML,NM} = 0.2355$ nm. We can see that, due to the FMS layer, the TMR is asymmetric, as a tunnel junction without a nonmagnetic layer is used. For each fixed voltage, the TMR oscillates, as is shown in figure 2(b) for $V_a = 50$ mV. The results show that more than 250% TMR can be obtained in reverse bias. By increasing the number of nonmagnetic monolayers, the TMR shows an oscillatory behaviour in the positive voltages. Under a forward bias, electrons at the Fermi energy of the left electrode tunnel into the empty states of the quantum well, which

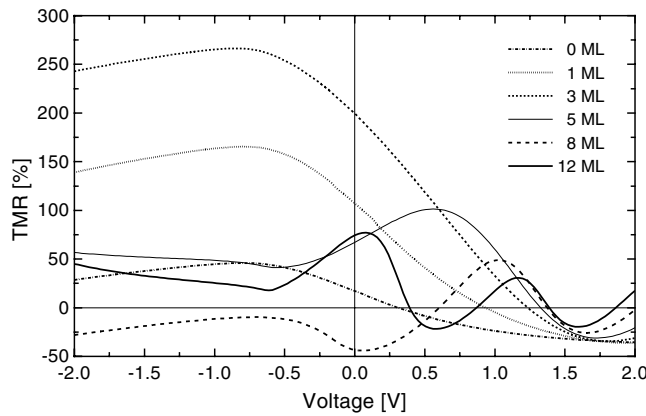


Figure 3. Dependence of the TMR on the applied voltage for different NM multilayers.

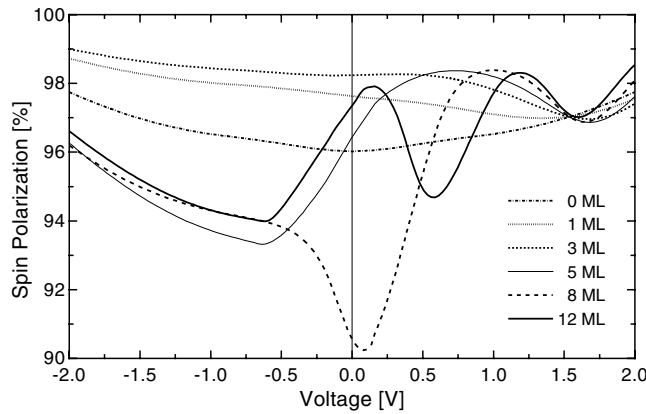


Figure 4. Dependence of the spin polarization on the applied voltage for different NM multilayers.

have been created due to the applied bias. Therefore the applied bias has a strong influence on the TMR and the oscillatory behaviour will appear. On the other hand, under a reverse bias, electrons at the Fermi energy of the quantum well tunnel into the empty states of the left electrode. In this case, variations of the applied bias cannot strongly affect the TMR.

In order to further see the effect of the FMS layer on the tunnel currents, we have shown in figure 4 the spin polarization of tunnelling electrons as a function of the bias voltage, for $t_{\text{ML,NM}} = 0.2355$ nm. It is obvious that the spin polarization is symmetric for $t_{\text{ML,NM}} = 0$, and becomes strongly asymmetric when the number of monolayers increases. The results show that the spin polarization can reach 99%, which is evidence of a spin filtering effect in the FMS layer.

The experimental measurements show that, if one uses a nonmagnetic insulator instead of a magnetic tunnel barrier, very low values for electron-spin polarization and TMR will result [7, 12]. The oscillatory behaviour of TMR, in terms of the NM layer thickness, is qualitatively in agreement with the experiments of Yuasa *et al* [12], and shows that the coherent tunnelling of electrons through the quantum well states is the main reason for this behaviour.

The present results can be qualitatively compared with those already known in the relevant literature, when a nonmagnetic barrier is used. In [13, 14], the authors showed that in the

FM/NM/I/NM/FM systems, the TMR in two different cases has an oscillatory behaviour with NM layers: the case where the thickness of both NM layers are equally varied (symmetric case), and the case where only one of the NM layers is increased (asymmetric case). In the symmetric case, the TMR is always positive, but in the asymmetric case the TMR oscillates from positive to negative as a function of the NM layer thickness. The situation in the asymmetric case is similar to our structure in which only one NM layer has been used [15]. Thus, as is clear from figures 2(b) and 3, our results are in qualitative agreement with the asymmetric case in FM/NM/I/NM/FM structures.

Finally, we discuss the effect of interface scattering on spin-injection from the FM into the NM spacer [31, 32]. For this purpose, we treated the magnetic barrier as a δ -function $U_\sigma \delta(x)$, with U_σ describing the barrier strength parameter for spin σ electron. In this case, the parameter U_σ is proportional to both the height and width of the barrier. The numerical results showed that with increasing the U_σ , the TC reduces, and hence the spin-dependent currents decay exponentially, which is due to the interface resistance. On the other hand, the spin polarization and TMR increase with U_σ , and tend gradually towards constant values, because in these values of the barrier parameter, only the FM electrodes have a dominant influence on the spin polarization and TMR.

4. Concluding remarks

The magnetotransport behaviour in FM/FMS/NM/FM tunnel junctions was investigated theoretically, using the transfer matrix method and the nearly-free-electron approximation. The numerical results indicate that in an Fe/EuS/Au/Fe structure, the TMR has an oscillatory behaviour as a function of the NM layer thickness. By increasing the thickness of the NM layer, both the TMR and electron-spin polarization oscillate under the forward biases. Due to the presence of a magnetic barrier, there exist more than 250% TMR and 98% spin polarization in the tunnel currents; this can be obtained by adjusting the thickness and the applied bias.

Our study was restricted to the zero temperature limit, because the ferromagnetic transition temperature in most of the FMS layers is much lower than room temperature [29]. Low temperature spin transport is, however, important as a testing ground for novel ideas and concepts in future spin electronic devices based on coherent transport [12, 33].

Acknowledgment

One of us (AAS) would like to express his sincere thanks to Professor K Esfarjani for illuminative comments.

References

- [1] Moodera J S, Kinder L R, Wong T M and Meservey R 1995 *Phys. Rev. Lett.* **74** 3273
- [2] Daughton J 1997 *J. Appl. Phys.* **81** 3758
- [3] Julliere M 1975 *Phys. Lett. A* **54** 225
- [4] Maekawa S and Gäfvert U 1982 *IEEE Trans. Magn.* **18** 707
- [5] Lu Y, Li X W, Gong G Q, Xiao G, Gupta A, Lecoeur P, Sun J Z, Wang Y Y and Dravid V P 1996 *Phys. Rev. B* **54** R8357
- [6] Seneor P, Fert A, Maurice J L, Montaigne F, Petroff F and Vaurès A 1999 *Appl. Phys. Lett.* **74** 4017
- [7] Moodera J S, Nowak J, Kinder L R, Tedrow P M, van de Veerdonk R J M, Smith B A, van Kampen M, Swagten H J M and de Jonge W J M 1999 *Phys. Rev. Lett.* **83** 3029
- [8] Sun J J and Freitas P P 1999 *J. Appl. Phys.* **85** 5264

- [9] LeClair P, Swagten H J M, Kohlhepp J T, van de Veerdonk R J M and de Jonge W J M 2000 *Phys. Rev. Lett.* **84** 2933
- [10] LeClair P, Kohlhepp J T, Swagten H J M and de Jonge W J M 2001 *Phys. Rev. Lett.* **86** 1066
- [11] Zhang S and Levy P M 1998 *Phys. Rev. Lett.* **81** 5660
- [12] Yuasa S, Nagahama T and Suzuki Y 2002 *Science* **297** 234
- [13] Vedyayev A, Ryzhanova N, Lacroix C, Giacomoni L and Dieny B 1997 *Europhys. Lett.* **39** 219
- [14] Wilczyński M and Barnaś J 2000 *J. Appl. Phys.* **88** 5230
- [15] Zhang W S, Li B Z and Zhang X 1998 *J. Appl. Phys.* **83** 5332
- [16] LeClair P, Ha J K, Swagten H J M, Kohlhepp J T, van de Vin C H and de Jonge W J M 2002 *Appl. Phys. Lett.* **80** 625
- [17] Filip A T, LeClair P, Smits C J P, Kohlhepp J T, Swagten H J M, Koopmans B and de Jonge W J M 2002 *Appl. Phys. Lett.* **81** 1815
- [18] Worledge D C and Geballe T H 2000 *J. Appl. Phys.* **88** 5277
- [19] Wilczyński M, Barnaś J and Świrkowicz R 2003 *J. Magn. Magn. Mater.* **267** 391
- [20] Saffarzadeh A 2003 *J. Phys.: Condens. Matter* **15** 3041
- [21] Saffarzadeh A 2004 *J. Magn. Magn. Mater.* **269** 327
- [22] Moodera J S, Hao X, Gibson G A and Meservey R 1988 *Phys. Rev. Lett.* **61** 637
Hao X, Moodera J S and Meservey R 1990 *Phys. Rev. B* **42** 8235
- [23] Fiederling R, Keim M, Reuscher G, Ossau W, Schmidt G, Waag A and Molenkamp L 1999 *Nature* **402** 787
- [24] Abramowitz M and Stegun I A 1965 *Handbook of Mathematical Functions* (New York: Dover)
- [25] Duke C B 1969 *Tunneling Phenomena in Solids* ed E Burstein and S Lundquist (New York: Plenum)
- [26] Rücker U, Demokritov S, Arons R R and Grünberg P 1996 *J. Magn. Magn. Mater.* **269/270** 156
- [27] Stearns M B 1977 *J. Magn. Magn. Mater.* **5** 167
- [28] Nolting W, Dubil U and Matlak M 1985 *J. Phys. C: Solid State Phys.* **18** 3687
- [29] Mauger A and Godart C 1986 *Phys. Rep.* **141** 51
- [30] Kittel C 1986 *Introduction to Solid State Physics* 6th edn (New York: Wiley)
- [31] Blonder G E, Tinkham M and Klapwijk T M 1982 *Phys. Rev. B* **25** 4515
- [32] Hu C M and Matsuyama T 2001 *Phys. Rev. Lett.* **87** 66803
- [33] Dietl T, Ohno H, Matsukura F, Cibert J and Ferrand D 2000 *Science* **287** 1019